Int. J. Electrochem. Sci., 15 **(2020)** 137 – 148, doi: 10.20964/2020.01.27

International Journal of
ELECTROCHEMICAL
SCIENCE
www.electrochemsci.org

Electrochemical Detection of Dopamine in Real Samples by an Indium Tin Oxide-Coated Glass Electrode Modified with Carbon Nanotubes

Bo Zhang[1,2*], *Qiong Wu*[1,2*], *Ben Li*[3*], *Xin Tang*[4], *Fei Ju*[2], *QianQian Yang*[2], *Qiuhong Wang*[2&], *You Lang Zhou*[2&]

[1] The Medical School of Nantong University, Nantong 226001, P.R. China.
[2] The Hand and Surgery Research Center, Department of Hand Surgery, Affiliated Hospital of Nantong University, Nantong 226001, P.R. China
[3]Department of Cardiothoracic Surgery, Affiliated Hospital of Nantong University, Nantong 226001, P.R. China.
[4] Key Laboratory of Neuroregeneration of Jiangsu and Ministry of Education, Co-Innovation Center of Neuroregeneration, Nantong University, Nantong 226001, P.R. China.
[*]These authors contributed equally to this study.
[&]E-mail: 18260599796@163.com, zhouyoulang@ntu.edu.cn

Received: 11 September 2019 / *Accepted:* 21 October 2019 / *Published:* 30 November 2019

The development of inexpensive and simple analytical tools is of practical significance for biological sample analysis. This work developed a simple and cost-effective electrochemical sensor that was covered with filter paper and modified by multi-walled carbon nanotubes (MWCNTs) for selective and sensitive dopamine (DA) detection in animal tissue extracts. We extracted animal tissue samples with an acidified n-butanol (1 ml/g) homogenate in an ice bath suitable for electrochemical detection. A DA response is received at a very low potential (0.43 V vs. Ag/AgCl) and is not affected by noradrenaline (NE) or 5-hydroxytryptamine (5-HT). We also investigated the correlation between analytical signals and the amount of assembled MWCNTs, as well as with the electrode area. The amperometric reaction to DA is found to be linear in a concentration range of 2.5×10^{-8} M to 1×10^{-5} M, with a 5 nM detection limit (signal-to-noise ratio of 3) under optimized experimental conditions. The method was further applied to quantify DA in the brain and tendon tissues of rats. The new method proposed is inexpensive, simple, and rapid compared to those of other conventional methods. It is pertinent to note that the sensor is a disposable, single-use sensor; thus, for every experiment, the electrode is prepared "as new". We presume that this approach is an effective mode for quantifying DA, which has great potential for future diagnostics of DA-related diseases.

Keywords: Dopamine; Electrochemical sensor; MWNTs; Diagnosis.

1. INTRODUCTION

Dopamine (DA), as a significant neurotransmitter, plays a crucial role in the central nervous system, along with the hormonal, cardiovascular, and renal systems [1]. Normally, the dopamine level in blood is very low and in the range of 0.01 to 1.0 μmol/L [2]. Increased concentrations of DA lead to numerous diseases, such as Huntington's disease, Alzheimer's disease, HIV infection, and Parkinson's disease [3-6], where dopamine activity is found to be lower than that in healthy individuals [7]. Hence, an accurate determination of DA has immense implications in the monitoring and diagnosis of disease. The conventional methods for the determination of DA include electrochemistry [8], chromatography [9], and enzymatic methods [10]. However, most of these methods require expensive instruments with time-consuming and tedious experimental steps, and sometimes the measurement results are inconsistent. Although a fluorescence (FL) probe method has been used by Zhou [11] and He [12] for the detection of DA, it was only capable of solving these problems to a certain extent. In the actual analysis, Zhou disclosed that it was difficult to acquire exact FL intensities because of the fluctuations in the reagent concentration and the inherent background FL. He developed a ratio-metric FL probe that used visual FL with naked-eye image recognition in DA analysis. The result was found to be subjective and difficult to apply for quantitative analysis.

In recent years, micro- and disposable analytical devices with excellent sensing capability have been developed for the detection of small molecules in biological samples [13-15]. Different from traditional electrochemical methods, the equipment mentioned above provides a powerful platform for analysis with the ability to reduce reagent consumption, analyse small sample sizes and reduce the processing time. Similar to our previous studies [16-18], indium tin oxide (ITO) was utilized as a substrate for the manufacture of disposable sensors because of its wide potential window, stable electrochemical performance, mass production and low cost.

A paper-based electrochemical sensor is described here that is used for the detection of DA and its quantification in the brain and tendon tissues of rats. The substrate electrode consisted of ITO and was modified by carboxylic multi-walled carbon nanotubes (MWCNTs). The detection of DA can reach a low of 5 nM with the use of a MWCNT/ITO coupled electrode as a paper-enabled analytical device for electrochemical sensing. This strategy is helpful in the bulk production of reproducible, cheap, and simple electrodes. Thus, the ease of handling and manipulation of the corresponding device, along with its miniaturization and disposable manner, can be improved in this way.

2. EXPERIMENTAL

2.1 Materials and reagents

From Sigma Aldrich (St Louis, MO, USA), we purchased the neurotransmitters DA, NE and 5-HT at analytical grade. From Nanbo Display Technology Co. Ltd. (Shenzhen, China), ITO conductive glass (355.6 × 406.4 × 1.1 mm STN, 10 Ω/cm^2) was purchased. Whatman No. 1 (Whatman grade 1 chromatographic paper) was purchased from Whatman International Ltd. (Maidstone, United Kingdom). The dispersion of 20.0 wt.‰ carboxylic MWCNTs (purity ≥95%, length: 0.5–2 μm, outer diameter > 50

nm) was obtained from Nanjing Xianfeng Nanomaterials Technology Co. Ltd. (Nanjing, China). An ITO chip was modified using MWCNTs diluted to 0.45 wt.‰. Different pH values of phosphate buffers (0.1 M) were made from NaH_2PO_4 and Na_2HPO_4 with their pH value adjusted by 0.1 M NaOH or H_3PO_4. Solutions of 5-HT, NE, and DA were made fresh daily with deoxygenated phosphate buffer solutions as a supporting buffer and diluted to the required concentration. Sprague-Dawley male rats (weight: 180–220 g, one month old) came from Nantong University Experimental Animal Center (Nantong, China). All solutions were prepared in double-distilled water (electrical resistivity was 18.0 MΩ cm).

2.2 Design and fabrication of the disposable electrode

With the intent to ensure sensor reproducibility (with a resistance value of 9.6–10.2 Ω/cm^2), a four-point probe technique (RTS-8) was applied to test the ITO chips for their electrical conductivity. To build the disposable electrodes, the ITO was cut into pieces of 20 mm×10 mm and ultrasonically cleaned with acetone, absolute ethanol and ultrapure water for 5 min, sequentially. Nitrogen gas was used for the drying process.

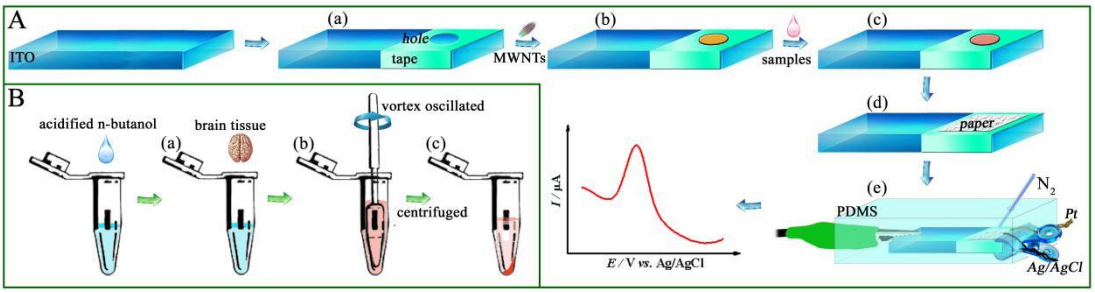

Scheme 1. (A) Step-by-step fabrication process of analytical devices and disposable electrodes. a A hole with diameter of 4 mm was drilled into plastic tape and then attached on the ITO chip. b 9 ml MWNTs were dripped on the 4 mm diameter of conductive zone and dried with nitrogen gas. c DA in phosphate buffer (pH 6.0, 10 uL) was dropped on the hole. D Cover the hole with a 6 mm long, 6 mm wide filter paper. The three-electrode electrochemical detection system: The PT and Ag/AgCl wires were integrated with ITO chip and PDMS cover. **(B)** Adding prepared brain tissue to precooled acidified n-butanol. B 5 min vortex oscillated. c centrifuged at 3 000 rpm for 5 min.

The manufacturing of the disposable electrode is detailed in Scheme 1 A (a) and (b). A hole with a diameter of 4 mm was drilled into plastic tape and then attached to the ITO chip, which provided the same electrode area for the disposable electrode used in the electrochemical experiments. 9 μL of MWCNTs (0.45 wt.‰) was dripped on a conductive zone of ITO glass that was 4 mm in diameter and then dried with nitrogen gas at room temperature for 15 min, completing the modification. These experimental conditions were detailed in our previous report [18], and some improvements were made (Fig. S1).

2.3 Electrochemical measurements

Electrochemical experiments were conducted at room temperature on a CHI1230B electrochemical workstation (CH Instruments Co., China). Scheme 1 A (c) to (e) illustrates the equipment integration and sample analysis process. The three-electrode system consists of ITO glass modified by MWCNTs as the working electrode, Ag/AgCl (4.8 cm long) as the reference electrode and platinum wire (4.8 cm long) as the auxiliary electrode. Before the three-electrode system was covered by PDMS and then formed as a paper-based analytical device, the sample (10 μL) was added to the electrode area, and filter paper (6 mm×6 mm) was placed on the electrode area. A thin-layer electrochemical cell was constructed using a piece of filter paper due to its porous structure. The working, counter and reference electrodes were electrically connected by the solution on the filter paper for electrochemical detection. The scanning electron microscopy (SEM) image was obtained with a JSM-6510 scanning electron microscope (JEOL Ltd., Japan) at an accelerating voltage of 5 kV.

2.4 Preparation of real samples

The real samples were taken from the brain and tendon tissues of rats. Scheme 1 B (a) to (c) illustrates the preparation process of rat brain tissue dispersions. After being anaesthetized with chloral hydrate (10%, 0.3 ml/100 g), the brain tissue was quickly removed and washed with precooled PBS 3 times, dried with filter paper, added to a precooled acidified n-butanol (1 ml/g) homogenate in an ice bath, vortexed for 5 min, and centrifuged for 5 min at 3000 rpm. The supernatants were obtained as an original rat brain grinding fluid containing NE, DA and 5-HT. As shown in Scheme 1 B (c), a 0.45 μm film was used to filter the supernatant, and then a phosphate buffer was used to dilute it (with the pH adjusted to 6.0) for the electrochemical assays. Then, the diluted supernatant was directly added (10 μL) as a droplet on the ITO surface and immediately scanned electrochemically by differential pulse voltammogram (DPV) and cyclic voltammogram (CV) methods. The tendon tissue was obtained from the Achilles tendon of the rat, and the method of making the sample was the same as that of the brain tissue.

3. RESULTS AND DISCUSSION

3.1 Characterization of the MWNTs/ITO

One of the important factors affecting the electrochemical response is the surface of the electrode. During the process of electrode preparation, we performed SEM to explore the difference between ITO and MWCNT/ITO. The SEM images of ITO and MWCNT/ITO are shown in Fig. 1. Obviously, the surface of ITO was smooth (Fig. 1A). On the MWCNT/ITO electrode surface, MWCNTs were uniformly distributed on the surface and existed in a single tube or small bundle form (Fig. 1B) These porous structures were favorable for the application of electrochemical analysis because their tridimensional structure not only increased the effective specific surface area of the electrode but also

acted as conduction channels for the rapid transmission of electrons and ions. The above may facilitate the effective transfer of electrons between the electrode and the substrate.

Cyclic voltammetry was utilized to measure the effective specific surface area at different scanning rates using ferric cyanide as a redox probe. As shown in Fig. S2, as the scanning rate increased from 30 to 400 mV/s, the peak potential slightly shifted, indicating some kinetic limitations [19]. In addition, the peak current linearly increased with the square root of the scan rate, indicating that the diffusion was controllable and that the process was reversible. The linear equation was $I_{pa}(A) = 3.96 \times 10^{-5}\ v^{1/2}$-$1.19 \times 10^{-4}$ ($R^2 = 0.9974$). We calculated the effective electrode area based on the Randles-Sevcik equation [20]:

$I_p=2.69\times10^5AD^{1/2}n^{2/3}v^{1/2}C$.

where A is the effective working area of the MWCNT/ITO electrode, C is the concentration of the redox probe, ν is the scan rate, D is the diffusion coefficient, and n is the number of electrons exchanged during the reaction.

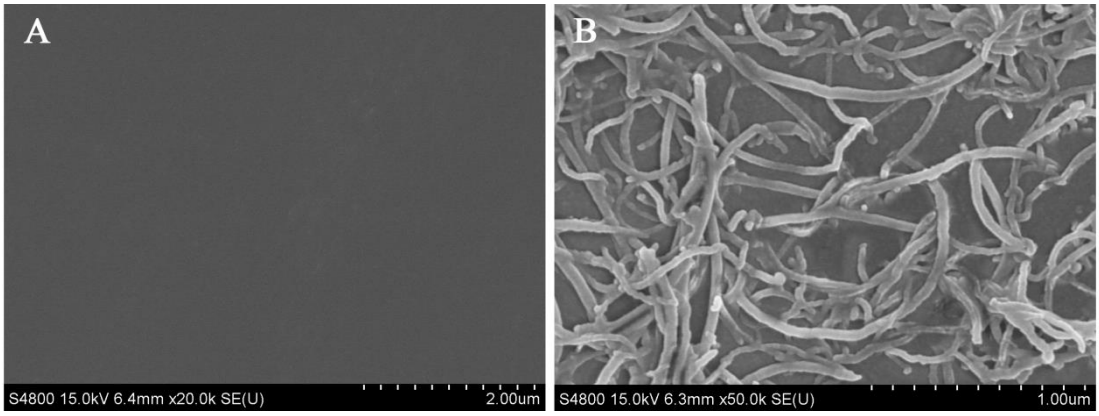

Figure 1. FE-SEM showed the ITO image (A) and MWNTs/ITO image (B)

From the slope of Ipa versus $v^{1/2}$, it was found that the MWCNT/ITO electrode effective area was 168.71 mm^2, which is 13.43 times as much as that of the bare ITO electrode (12.56 mm^2) and much larger than that of MWCNT/NF/ITO (19.63 mm^2) [21] electrodes. This meant that the tridimensional structure of MWCNTs increased the active surface area of the working electrode. In comparison to conventional methods, the proposed method is simple, rapid and inexpensive.

3.2 Electrochemical behavior of DA at MWNTs/ITO

CV was used to investigate the electrochemical behavior of DA with the MWCNT/ITO electrode. As shown in Fig. 2, we compared the cyclic voltammograms for DA oxidation with different electrodes. No electrocatalytic oxidation peak was observed with the ITO and MWCNT/ITO electrodes when DA was absent in pH 6.0 phosphate buffer (Fig. 2A). The current of the MWCNT/ITO electrode was found to be higher in the presence of 1 mM DA than that with a bare ITO electrode, and large shifts were noticed in the peak potentials (Fig. 2B).

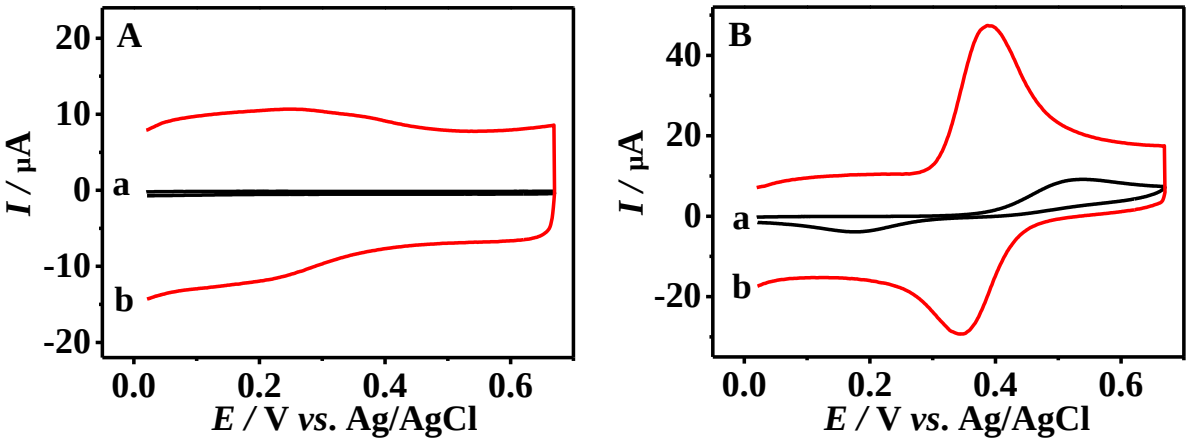

Figure 2. (A) Cyclic voltammograms were utilized to investigate the DA electrochemical behavior at different electrodes in pH 6.0 phosphate buffer.(ITO: a; MWNTs/ITO: b) **(B)** In the presence of I mM DA, the current at MWNTs/ITO was found to be higher than at bare ITO. (50 mV s^{-1} ccan rate; ITO: a; MWNTs/ITO: b)

This result indicates that higher numbers of MWCNTs in solution would provide wider surface area for efficient DA binding [22]. It should be noted that the redox peaks having a 0.34 V separation appeared in a well-defined manner on the MWCNT/ITO electrode (Fig. 2B a), illustrating that the DA reversibility was superior to that of the bare ITO electrode (ΔE=365 mV). This paired redox peak corresponded to a two-electron oxidation of DA to dopamine quinone, eventually reducing the dopamine quinone into DA [23].

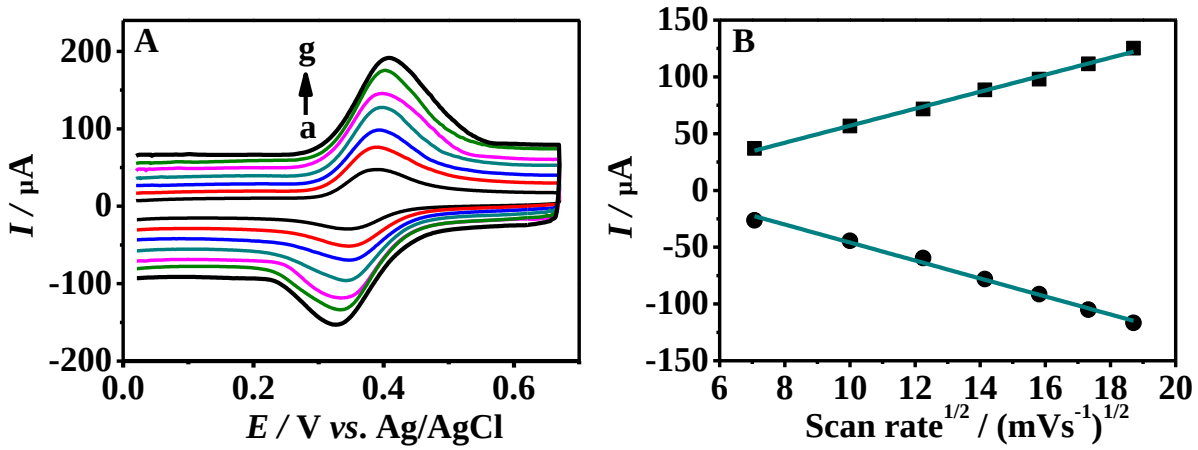

Figure 3. (A) The CVs of MWNTs/ITO electrode in 1 mM DA in different scan rates. (a − g: 50 - 350 mV s^{-1}, 50 mV s^{-1} for an interval). **(B)** Plot of peak current vs. Scan $rate^{1/2}$.

A controlling step in the oxidation of DA is indirectly shown by the relationship between the redox currents and the scan rates. The CV presence of the MWCNT/ITO electrode in 1 mM DA with scan rates ranging from 50 to 350 mV s^{-1} is expressed in Fig. 3. The anodic peaks were observed to shift in the positive direction, whereas the peaks of the cathode tended to slightly shift in the negative

direction, thereby indicating a quasi-reversible electrode reaction for DA. Both the cathodic and anodic peaks change currents with the increase in scan rates, indicating a linear correlation with the square root of the scan rates (Fig. 3B). The linear equations of the square root vs. the peak current are depicted as Ipa (μA) = 7.49×10^{-6} $v^{1/2}$-1.79×10^{-5} (R^2 = 0.9950), for the anodic peak currents, and Ipc (μA) =-7.92×10^{-6} $v^{1/2}$ +$3.33 \times 10-5$ (R^2 = 0.9939), for the cathodic peak currents. This finding indicates that the redox of DA at the MWCNT/ITO electrode is a typical diffusion-controlled process, which is consistent with the observations of the dopamine oxidation and reduction process with MWCNTs by N. G. Tsierkezos [24] and Q. M. Feng [21].

3.3 Effects of the solution pH

The influence of the solution pH on the peak potentials and peak currents of DA oxidation was investigated by DPV with a pH range of 4.0 to 8.0 (Fig. 4). It was found that the current intensity and peak potential depend significantly on the pH range from 4.0 to 8.0, indicating the role of protons in the DA oxidation process. This was the result of de-protonation steps involved in all oxidation processes, which could be easily carried out at higher pH values. Since the DA charging state and the H^+ strength vary with pH difference, the peak potentials turn into negative values when the solution pH increases. The peak potential of DA as a function of the solution pH with its linear regression equation is shown in Fig. 4B and can be expressed as follows:

Epa (DA) = −0.05804pH + 0.7805 (R^2 = 0.9980)

The linear pH dependence is shown by the formal potential, with a slope (58.04 mV pH^{-1}) near that of the Nernst system (59 mV/pH at 25 ° C); The above results confirm equal amounts of protons and electrons are involved in the electrode reaction, which is in agreement with the previously reported mechanism of DA oxidation [25,26].

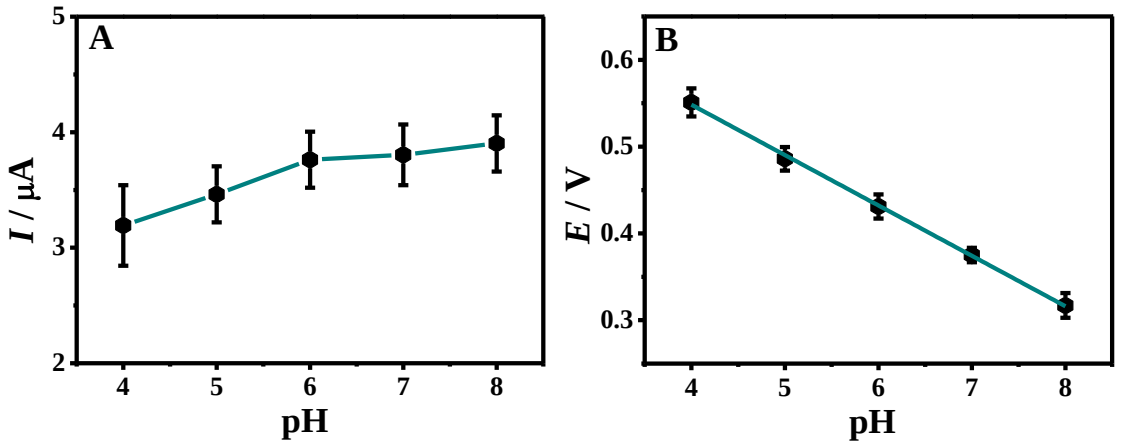

Figure 4. (A) Plots of Ipa vs. pH. **(B)** Plots of E vs. pH (n=3).

It is evident from Fig. 4A that the oxidation peak current for DA was observed to increase up to pH 8.0 as deprotonation did not occur at a solution pH<8.0. A PBS pH of 6.0 was identified for the analysis in view of the separation effect and detection sensitivity.

3.4 Detection of DA at the disposable electrode

A differential pulse voltammogram with low detection and a highly sensitive electrochemical approach was applied to determine the properties of the sensor on the oxidation of DA under optimum conditions. The DPV curves with different concentrations of DA at the MWCNT/ITO electrode are shown in Fig. 5A. With increasing DA concentration, the peak current significantly increased. In a wide range (2.5×10^{-8} to 10^{-5} M), the oxidation peak currents of DA are proportional to its concentration. The linear equation was $I_p(\mu A) = 0.37256C_{DA}(\mu M) + 2.2707 \times 10^{-8}$($R^2 = 0.9948$) (Fig. 5B). The detection limit was estimated to be 5 nM.

Table 1. Summary of comparison on the performance between the electrochemical detection of DA and electrodes modified by other materials

Electrode	**Technique**	**Linear range(μM)**	**LOD(μM)**	**Electrolyte**	**Interferents**	**Reference**
GR-CS/GCE	DPV	0.03-20.06	0.0045	PBS(7.0)	AA, UA	[20]
MWCNTs/NF/ITO	DPV	0.01–1	0.01	PBS(7.4)	–	[21]
MXene/DNA/Pd/Pt/GCE	DPV	0.2-1000	0.03	PBS(7.0)	AA, UA, Glu	[22]
MWCNT-BZ	DPV	0.17–3	0.03	PBS(7.0)	–	[24]
ITO	LSV	0.001–0.1	0.001	Tris buffer(9.5)	–	[25]
rGO-CNT/ITO	DPV	0.8 – 8	0.04	PBS(7.0)	AA, UA,	[27]
Au/AGR/MWCNT	CV, SWV	1.0 – 210	0.08	PBS(7)	AA, UA, FA	[28]
PEDOT /ITO	DPV	1–50	6.77	PBS(7.4)	AA	[29]
Tyrosinase/NiO/ITO	CV	2–100	0.06	PBS(6.5)	AA, UA	[30]
DyHCF/fMWCNTs/GCE	DPV	3–289	–	PBS(7)	AA, UA	[31]
AuNP/Pd	SWV	0.5–1000	0.008	PBS(7.2)	UA, 5-HT	[32]
ITO-PDA-AuNP	DPV	4–200	0.06	PBS(7.0)	AA	[34]
MWNTs/ITO	DPV	0.025–10	0.005	PBS(6.0)	NE, 5-HT	This work

BZ benzene; GCE glassy carbon electrode; GR graphite; CS chitosan; PDA Polydopamine; AuNPs gold nanoparticles; NF Nafion; rGO reduced graphene oxide; CNT carbon nanotube; AGR activated graphene; PEDOT poly (3, 4 ethylenedioxythiophene); NiO Nickel oxide; DyHCF dysprosium hexacyanoferrate

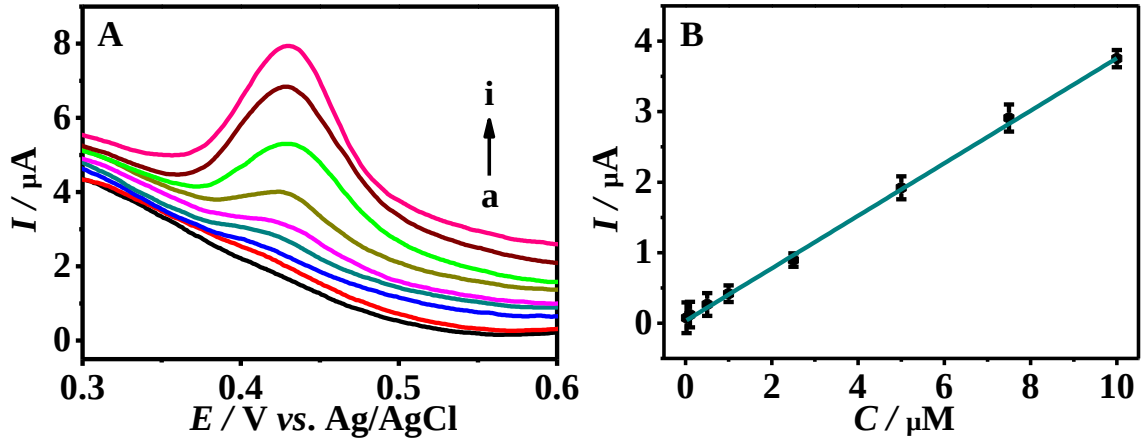

Figure 5 (A) DPV curve of DA in different concentrations of pH 6.0 PBS.(a–h: 0, 0.025, 0.1, 0.5, 1, 2.5, 5, 7.5 and 10 μM) **(B)** Plot of the peak current against DA concentration (n=3).

The major performance of the sensor in DA detection was comparable with that of several other sensors (Table 1). The comparison shows that the detection limit is lower and the linear range is wider than those of other sensors. However, the detection limit is not the best. A wide linear range and a low detection limit are helpful in developing further applications in real sample analysis. Moreover, it could be seen that other sensors were engaged to detect blood samples that were treated or injected, while modified sensors were first used for monitoring the brain tissue of rats.

These results confirmed the efficiency of MWCNT/ITO as a media for a less electrocatalysing approach of DA analysis. In addition, it should be noted that every electrode used in this work was used just once, and all experimental data were an average of the obtained results from three different electrodes. Therefore, electrode fouling, which is commonly encountered with conventional solid electrodes for the oxidation of DA, can be evaluated. The reproducibility of the sensor was of great importance to the characteristics of its one-time use. Under the same experimental conditions, the relative standard deviation of 50 μM DA was approximately 8.26%, which indicated that the method has good reproducibility.

3.5 Real sample analysis and interferences

The as-prepared electrode was utilized to determine DA in rat brain and tendon tissue samples with an intent to evaluate the feasibility of the MWCNT/ITO electrode in real sample analysis. The DPV was enumerated from -0.5 to 0.7 V at a 100 mV/s scan rate. As shown in Fig. 6A, a curve was obtained with 100 μL of initial rat brain grinding liquid that was diluted to 400 μL with a buffer solution. The oxidation peaks of DA can be observed. As different volumes of DA (5×10^{-7} M, 10^{-6} M, 2.5×10^{-6} M, 4×10^{-6} M, 5×10^{-6} M) were added to the diluted brain tissue sample, the standard curve for real samples could be observed (Fig. 6A inset). The linear equation is Ip (μA) = $0.3745C_{DA}$(M) $+3.0334\times10^{-7}$ (R = 0.99602). This suggests that DA levels in brain tissue can be accurately detected, and the electrode can

provide a detection basis for the dopamine changes in real samples caused by disease or environmental changes.

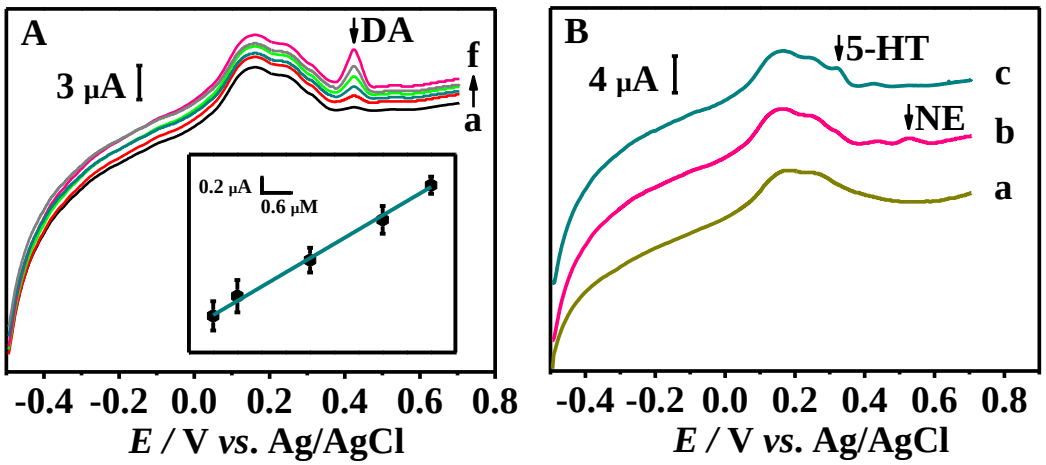

Figure 6. (A) DPV curves of different volumes of DA(0 M, 5×10^{-7} M, 10^{-6} M, 2.5×10^{-6} M, 4×10^{-6} M, 5×10^{-6} M) was added to the diluted brain tissue sample(PH=6.0), Inset: Plot of the peak current against the DA concentration. **(B)** DPV curves of diluted tendon tissue sample (PH=6.0) (a). DPV curves of different volumes of 5 μM NE (b), 5 μM 5-HT (c) were added to the diluted brain tissue sample3 (PH=6.0) (n=3).

Subsequently, the simultaneous electrochemical detection of 5-HT, DA and NE was examined by using DPV. Fig. 6B shows the DPV curve of the diluted tendon tissue sample (a) and the DPV curves of the MWCNT/ITO electrode in the diluted brain tissue sample containing 5 μM NE (b) and 5 μM 5-HT (c). The oxidation of 5-HT, DA and NE with the MWCNT/ITO electrode can be identified, and three oxidation current peaks of DPV are attributed to the oxidation of 5-HT (0.32 V), DA (0.43 V) and NE (0.52 V). This result indicates that the MWCNT/ITO electrode can simultaneously detect NE, 5-HT and DA at relatively low concentrations using DPV.

In addition, Fig. 6B shows that a low-concentration (5 μM) of NE and 5-HT is maintained in the background and is unchangeable; in contrast, the concentration of DA remains constant at 0.2 μM. Therefore, the peak current of DA was influenced, but the result was less than ±5%, which was within the error allowed. As reported, the basal DA concentration is very low (110.33±10.56 $ng\cdot g^{-1}$), while the concentration of NE and 5-HT is much lower (70.05±6.28 $ng\cdot g^{-1}$ and 50.12±6.85 $ng\cdot g^{-1}$) in the rat brain [35]. Hence, in actual detection, the effects would be small. Compared with Feng [21], our method effectively eliminates the interference of a low concentration of NE and 5-HT in real samples for DA detection. The results demonstrated that MWCNT/ITO showed impressive anti-interference capability in the case of the concurrent determination of DA in a complex sample.

4. CONCLUSIONS

During the study, an innovative and ingeniously developed modified disposable electrode was successfully applied for determining DA in detection samples. The modified electrode yielded the

effective separation of DA, NE and 5-HT oxidation peaks. The newly developed sensor incorporated the benefits of MWCNT/ITO, providing an innovative method for the continuous determination of DA in actual samples with high stability, selectivity, and sensitivity. As ITO is low cost and reproducible, it provides an incredibly easy approach for clinical diagnosis on the spot. The materials can be conveniently assembled into sensing devices with portable chips appropriate for handling by unskilled staff or assembled into a portable chip sensor device that is suitable for non-technical users.

ACKNOWLEDGMENTS
National Natural Science Foundation of China (81401796, 51603106 and 81771999) and the National Undergraduate Training Programs for Innovation (Nantong university, 201910304030Z; 201910304028Z) supported this work.

CONFLICTS OF INTEREST
None

References

1. M. Sajid, M.K. Nazal, M. Mansha, A. Alsharaa, S.M.S. Jillani and C. Basheer, *Trac-trend. Anal. Chem.*, 76 (2016) 15.
2. R.P. da Silva, A.W.O. Lima and S.H.P. Serrano, *Anal. Chim. Acta.*, 612 (2008) 89.
3. V. Wang, T.H. Chao, C.C. Hsieh, C.C. Lin and C.H. Kao, *Parkinsonism Relat D.*, 21 (2015) 18.
4. P. J. Gaskill, T.M. Calderon, A.J. Luers, E.A. Eugenin, J.A. Javitch and J.W. Berman, *Am. J. of Pathol.*, 175 (2009) 1148.
5. A. Petersén, K.E. Larsen, G.G. Behr, N. Romero, S. Przedborski, B. Brundin and D. *Sulzer, Hum. Mol. Genet.*, 10 (2001) 1243.
6. S. Reeves, E. Mclachlan, J. Bertrand, F. D'Antonio, S. Brownings, A. Nair, S. Greaves, A. Smith, D. Taylor, J. Dunn, P. Marsden, R. Kessler and R. Howard, *Brain*, 140 (2017) 1117.
7. N.G. Mphuthi, A.S. Adekunle, O.E. Fayemi, L.O. Olasunkanmi and E.E. Ebenso, *Sci. Rep.*, 7 (2017) 43181.
8. T. Qian, C.F. Yu, X. Zhou, P.P. Ma, S.S. Wu, L.N. Xu and J. Shen, *Biosens. Bioelectron.*, 58 (2014) 237.
9. K. Syslova, L. Rambousek, M. Kuzma, V. Najmanova, V.B. Valesova, R. Slamberova and P. Kacer, *J. Chromatogr. A.*, 1218 (2011) 3382.
10. M.B. Fritzen-Garcia, F.F. Monteiroa, T. Cristofolini, B.G. Zanetti-Ramos, V. Soldi, A.A. Pasa and T.B. Creczynski-Pasa, *Sensor Actuat. B-Chem.*, 182 (2013) 264.
11. X. Zhou, P.P. Ma, A.Q. Wang, C.F. Yua, T. Qian, S.S. Wu and J. Shen, *Biosens. Bioelectron.*, 64 (2015) 404.
12. W.J. He, R.J. Gui, H. Jin, B.Q. Wang, X.N. Bu and Y.X. Fu, *Talanta*, 178 (2017) 109.
13. A. Jodra, M. Hervás, M.Á. López and A. Escarpa, *Sensor Actuat. B-Chem.*, 221 (2015) 777.
14. C.M. Yu, Z.K. Zhu, L.Wang, Q.H.Wang, N. Bao and H.Y. Gu, *Biosens. Bioelectron.*, 53 (2014) 142.
15. B.X. Shi, Y. Wang, K. Zhang, T.L. Lam and H.L. Chan, *Biosens. Bioelectron.*, 26 (2011) 2917.
16. C.M. Yu, Q.H.Wang, D.P. Qian, W.B. Li, Y. Huang and F.T. Chen, N. Bao and H.Y. Gu, *Microchim. Acta.*, 183 (2016) 3167.
17. Q.H. Wang, W.B. Li, D.P. Qian, Y.B. Li, N. Bao, H.Y. Gu and C.M. Yu, *Electrochim. Acta*., 204 (2016)128.
18. Q.H. Wang, W.B. Li, N. Bao, C.M. Yu and H.Y. Gu, *Microchim. Acta.*, 183 (2016) 423–430.
19. X.Y. Zhao, H.F. Jia, J.B. Kim and P. Wang, *Biotechnol. Bioeng.*, 104 (2009) 1068.

20. S. Palanisamy, K. Thangavelu, S.M. Chen, P. Gnanaprakasam, V. Velusamy and X.H. Liu, *Carbohyd. Polym.*, 151 (2016) 401.
21. Q.M. Feng, M. Cai, C.G. Shi, N. Bao and H.Y. Gu, *Sensor. Actua.t B-Chem.*, 209 (2015) 870.
22. Z. Herrasti, F. Martínez and E. Baldrich, *Sensor. Actuat. B-Chem.*, 203 (2014) 891.
23. R. Trouillon, D. O'Hare, *Electrochim. Acta.*, 55 (2010) 6586.
24. N.G. Tsierkezos, U. Ritter, *J. Solid. State. Electr.*, 16 (2012) 2217.
25. S.K. Yadav, Rosy, M. Oyama. and R.N. Goyal, *J. Electrochem. Soc.*, 161 (2014) H41.
26. C.L. Sun, H.H. Lee, J.M. Yang and C.C. Wu, *Biosens. Bioelectron.*, 26 (2011) 3450.
27. Y. Zhang, Y. Ji, Z. Wang, S. Liu and T. Zhang, *Rsc. Adv.*, 5 (2015) 106307.
28. A.A. Abdelwahab, Y.B. Shim, *Sensor Actuat. B-Chem.*, 221 (2015) 659.
29. R.K. Pal, S.C. Kundu and V.K. Yadavalli, *Sensor Actuat. B-Chem.*, 242 (2017) 140.
30. A. Roychoudhury, S. Basu, S.K., *Biosens. Bioelectron.*, 84 (2016) 72.
31. B. Devadas, S.M. Chen and M. Rajkumar, *Electrochim. Acta.*, 105 (2013) 439.
32. B.K. Kim, Y.L. Ji, J.H. Park, J. Kwak, *J. Electroanal. Chem.*, 708 (2018) 7.
33. B. Devadas, S.M. Chen and M. Rajkumar, *Electrochim. Acta.*, 105 (2013) 439.
34. H. Zhang, F. Zhang, S. Li and H. Li, *Ionics*, 23 (2017) 2475.
35. B. Michaelidis, N.S. Loumbourdis and E. Kapaki, *J. Exp. Biol.*, 205 (2002) 1135.